Yathavan, K and Stacey, T R, Laboratory observations relevant to fracture initiation at low stress levels
SANIRE 2004 – The Miner's Guide through the Earth's Crust, South African National Institute of Rock Engineering

Laboratory observations relevant to fracture initiation at low stress levels

K Yathavan and T R Stacey
University of the Witwatersrand

Rock fracture at low stress levels can be a source of unexpected problems in rock engineering - safety hazards, unexpected support requirements, more difficult excavation conditions, longer construction times and ultimately higher costs. Therefore, the understanding of the mechanism of fracture initiation is essential for the "correct" design of underground excavations.

This paper highlights some laboratory experimental work on anorthosite and sandstone samples to determine the fracture initiation point using stress-strain graphs. Detailed scanning electron microscope studies of the above samples show some fascinating fracture processes and fracture patterns developed at low stress levels.

The authors believe that this experimental work could contribute towards the understanding of some fundamental aspects of fracture mechanics, as well as towards rock engineering in general.

Introduction

Rock fracture at low stress levels can be a source of unexpected problems in rock engineering - safety hazards, unexpected support requirements, more difficult excavation conditions, longer construction times and ultimately higher costs (Stacey and Yathavan, 2003). Therefore, the understanding of the mechanism of fracture initiation is essential for the “correct” design of underground excavations.

Brace and Bombolakis (1963) and Bieniawski (1967a, 1967b) studied the deformation and fracture characteristics of brittle rock in detail. Their studies, based on the concepts of Griffith cracks or flaws, show that the failure process can be divided into five stages: (I) crack closure, (II) linear elastic deformation, (III) crack initiation and stable crack growth, (IV) critical energy release and unstable crack growth, (V) failure and post peak behaviour. These failure processes are divided on the basis of stress-strain characteristics determined from axial and lateral deformation measurements recorded during uniaxial and triaxial laboratory tests. Figure 1 (Martin and Chandler, 1994) gives a detailed explanation of the above five stages.

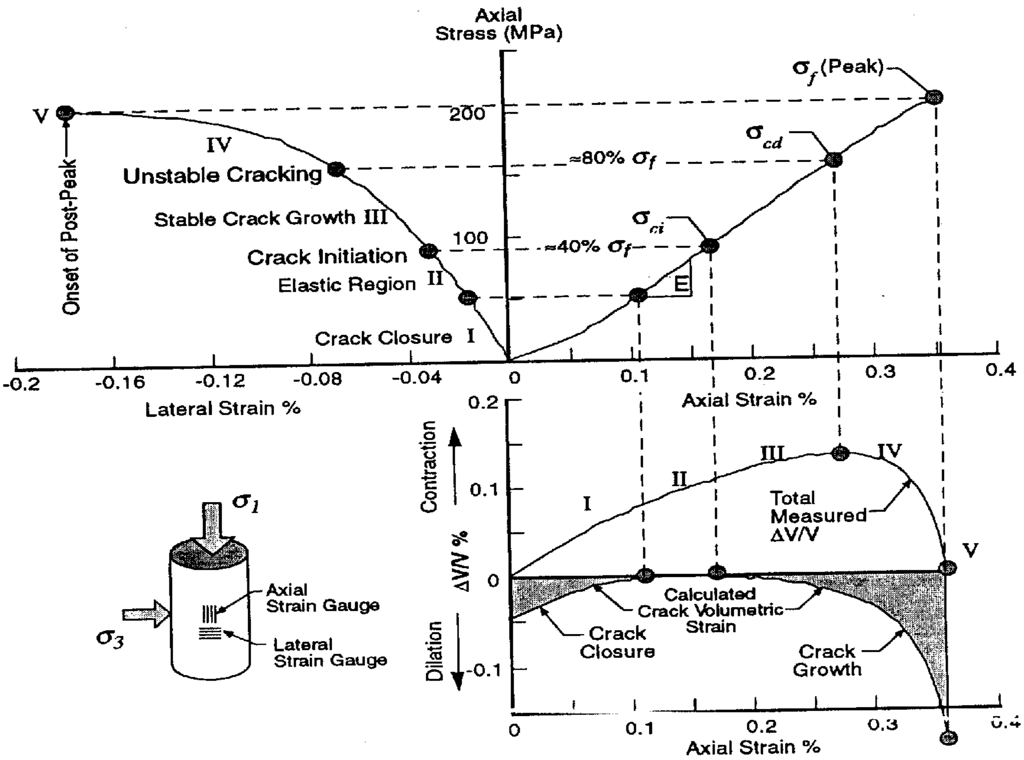

Figure 1: Stress strain diagram obtained from a single uniaxial compression test showing the definition of crack initiation (σ_{ci}), crack damage (σ_{cd}) and peak strength (Martin and Chandler, 1994).

During crack closure, the stress-strain response is non-linear; exhibiting an increase in axial stiffness, and some sliding between the faces of closed cracks may take place. The extent of this non-linear region is dependent on the initial crack density and geometrical characteristics of the crack population. Linear elastic deformation takes place when the majority of pre-existing cracks have closed.
Microcracking begins at the stress level at which cracks initiate, which is called the crack initiation stress level (σ_{ci}). At this point the lateral and volumetric strain curves depart from linearity as shown at point A in Figure 2 (Brace et al, 1966; Bieniawski, 1967).

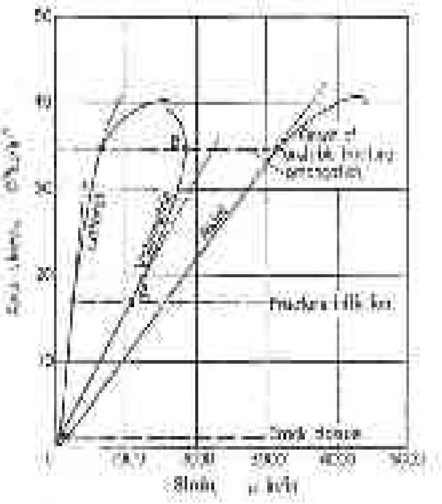

Figure 2: Relationship between axial stress and axial, lateral and volumetric strain (Bieniawski, 1967a and 1967b).

Fracture initiation and unstable fracture propagation stress levels are found to be independent of the shapes of specimens, loading patterns and testing machines as investigated in microscopic examination of thin sections from the specimens loaded to various stress levels by Bieniawski (1967a, 1967b). Crack initiation is difficult to identify in laboratory stress strain curves, especially if the sample already contains a high density of microcracks. Therefore Martin and Chandler (1994) defined crack initiation as the stress level at which dilation (crack volumetric strain increase) just begins on a plot of crack volumetric strain. For a cylindrical sample subjected to axial loading, with or without confining stress, and under small strains, the volumetric strain (ε_v) is given by

$$\varepsilon_v = \frac{\Delta V}{V} \approx \varepsilon_{axial} + 2\varepsilon_{lateral} \qquad (1)$$

The crack volumetric strain is found by subtracting the elastic volumetric strains from the total volumetric strains. The elastic volumetric strains are calculated using the elastic constants determined from the linear portion of stress strain curves in Region II as shown in Figure 1.

$$\frac{\Delta V}{V_{elastic}} = \frac{1-2\nu}{E}(\sigma_1 - \sigma_3) \qquad (2)$$

The following table summarises the procedure for obtaining σ_{ci} values from the laboratory test results.

	Identifying methods	Crack closure, σ_{cc}	Crack Initiation, σ_{ci}	Crack Coalescence, σ_{cs}	Crack damage, σ_{cd}
Brace, Brace et al, 1963; Bieniawski (1967a, 1967b)	Axial strain	Point of non-linear zone changes to linear zone	-	-	-
	Lateral strain	-	Point of departure from linearity to non-linearity	-	-
	Volumetric strain	-	Point of departure from linearity to non-linearity	-	Point of reversal
Martin and Chandler(1994)	Crack Volumetric strain	-	Dilation begins after crack volume unchanged during elastic deformation	-	-

Table1: Method of stress threshold identification methods based on stress-strain curves

Experimental Procedure

Rock Samples

Laboratory tests were carried out at the University of Witwatersrand to investigate the mechanical properties of 42mm diameter anorthosite core samples and dry drilled 42mm diameter sandstone samples. In all cases ISRM (1979) suggested methods were followed to determine the mechanical properties. The results of the tests are summarized in Table 2.

Sample	Anorthosite		Sandstone	
Property	Range	Average	Range	Average
Uniaxial Compressive Strength (MPa)	77.23 - 110.43	93.95	18.9 -23.12	21.08
Young's Modulus (GPa)	16.4 - 32.38	22.72	3.19 -5.33	4.16
Poisson's Ratio	0.15 - 0.34	0.21	0.26 - 0.47	0.35
Brazilian Tensile Strength (MPa)	2.7 - 9.1	5.3	0.72 - 1.30	0.9

Table 2: Mechanical properties of the anorthosite and sandstone samples

By plotting the measured axial and lateral strains, and the calculated volumetric strains, against the applied axial stress, the path of a rock sample to failure can be followed.

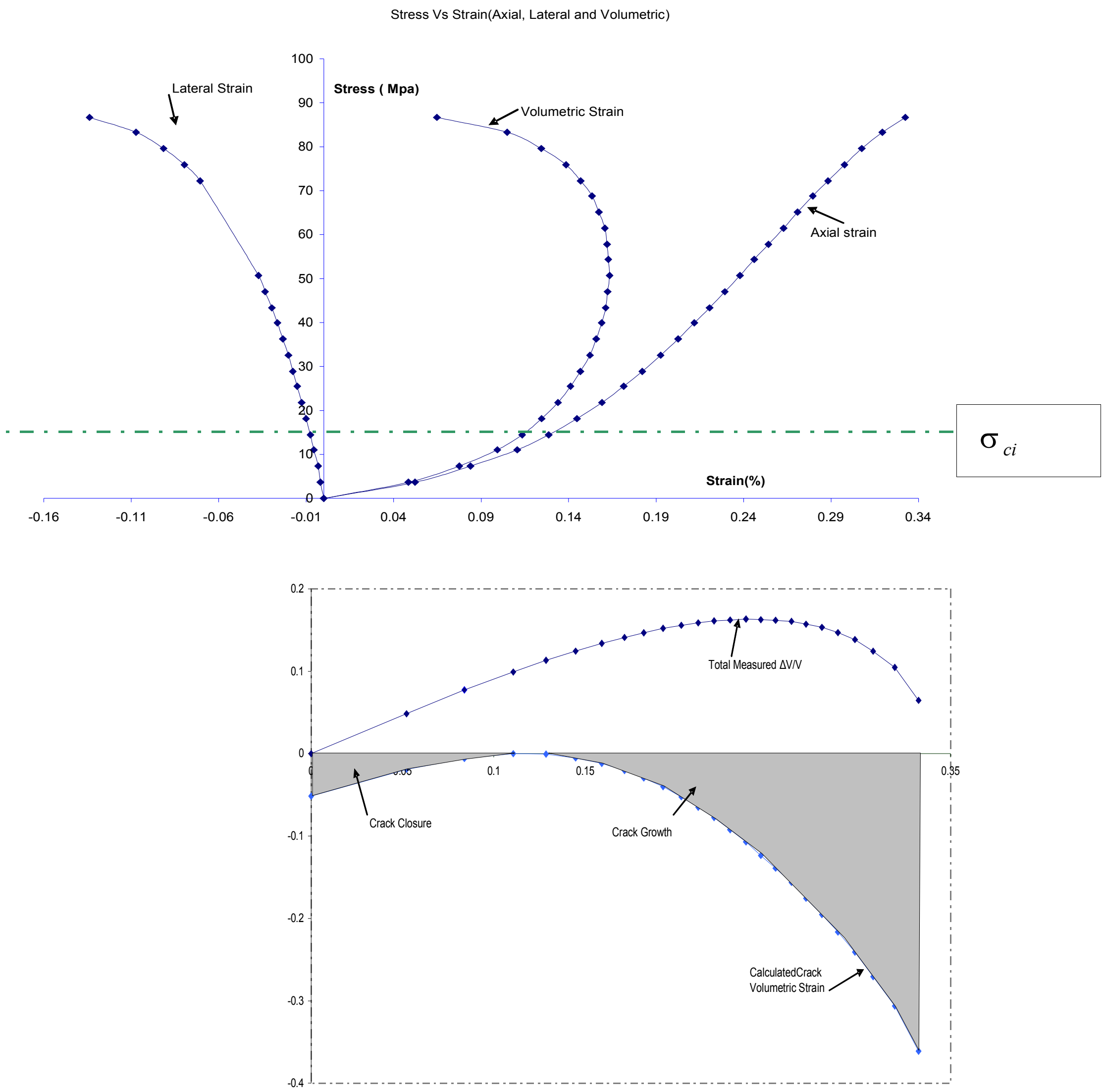

Figure 3: Stress-strain graph obtained from a single uniaxial compression test on anorthosite.

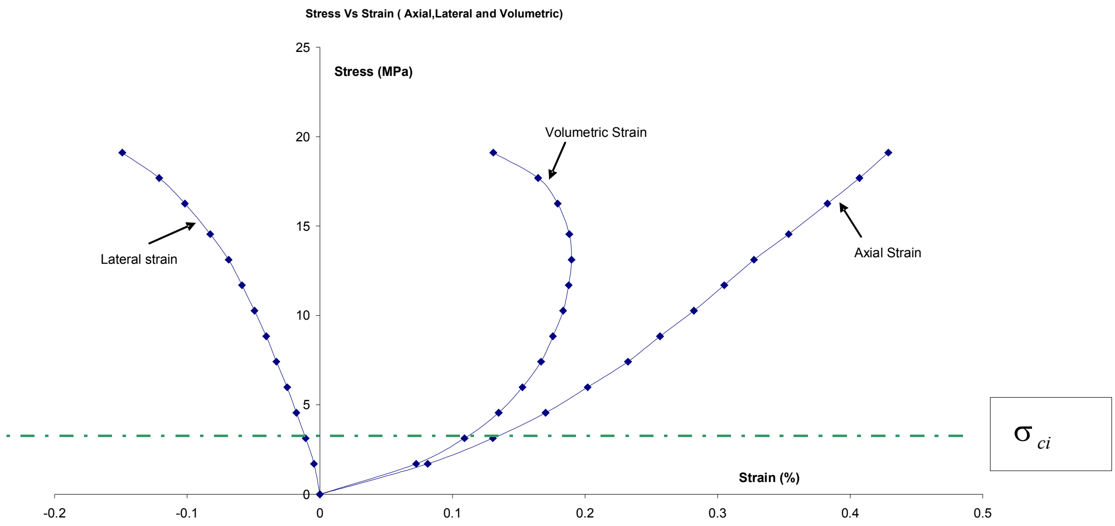

Figure 4: Stress-strain graph obtained from a single uniaxial compression test on sandstone.

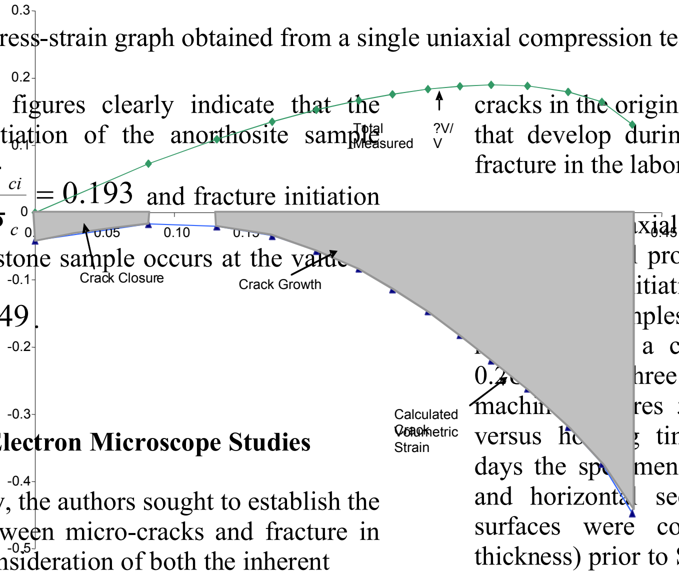

The above figures clearly indicate that the fracture initiation of the anorthosite sample occurs at $\frac{\sigma_{ci}}{\sigma_c} = 0.193$ and fracture initiation of the sandstone sample occurs at the value $\frac{\sigma_{ci}}{\sigma_c} = 0.149$.

Scanning Electron Microscope Studies

In this study, the authors sought to establish the relation between micro-cracks and fracture in rocks by consideration of both the inherent cracks in the original rock and the micro-cracks that develop during the processes leading to fracture in the laboratory.

[illegible] axial compressive strength test, [illegible] properties of each sample and [illegible] initiation point were determined. [illegible] ples of the two rock types were [illegible] a compressive stress level of 0.2[illegible] three days in an MTS testing machin[illegible] res 5 and 6 illustrate the load versus ho[illegible] time characteristics. After 3 days the sp[illegible] men was unloaded and vertical and horizontal sections prepared. Specimen surfaces were coated with carbon (200Å thickness) prior to SEM observation in order to prevent surface charging under the electron beam.

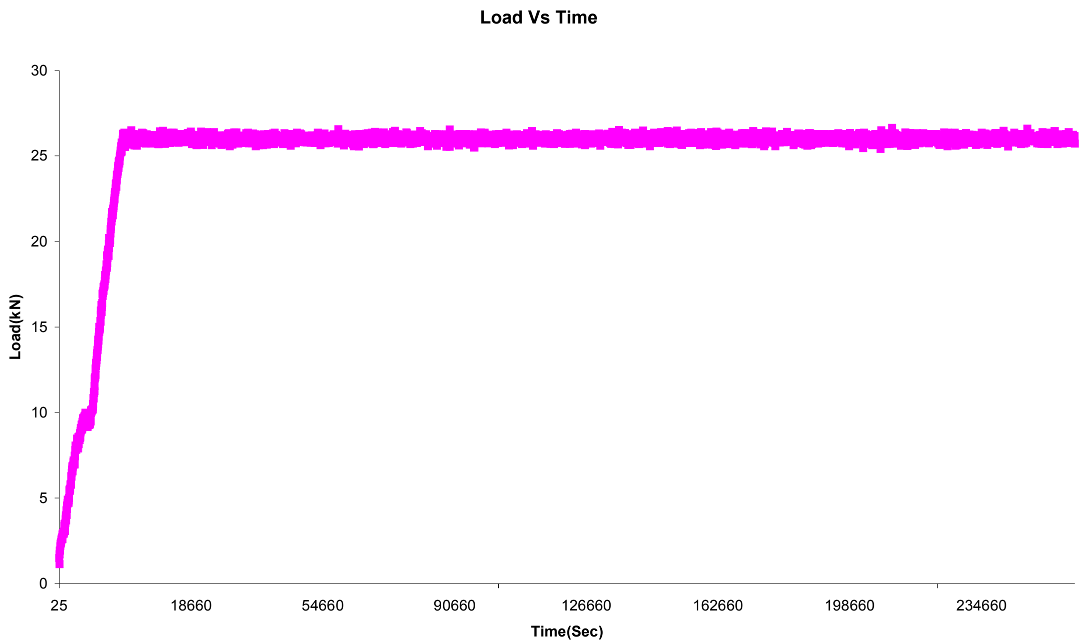

Figure 5: Load-time characteristic for anorthosite rock sample

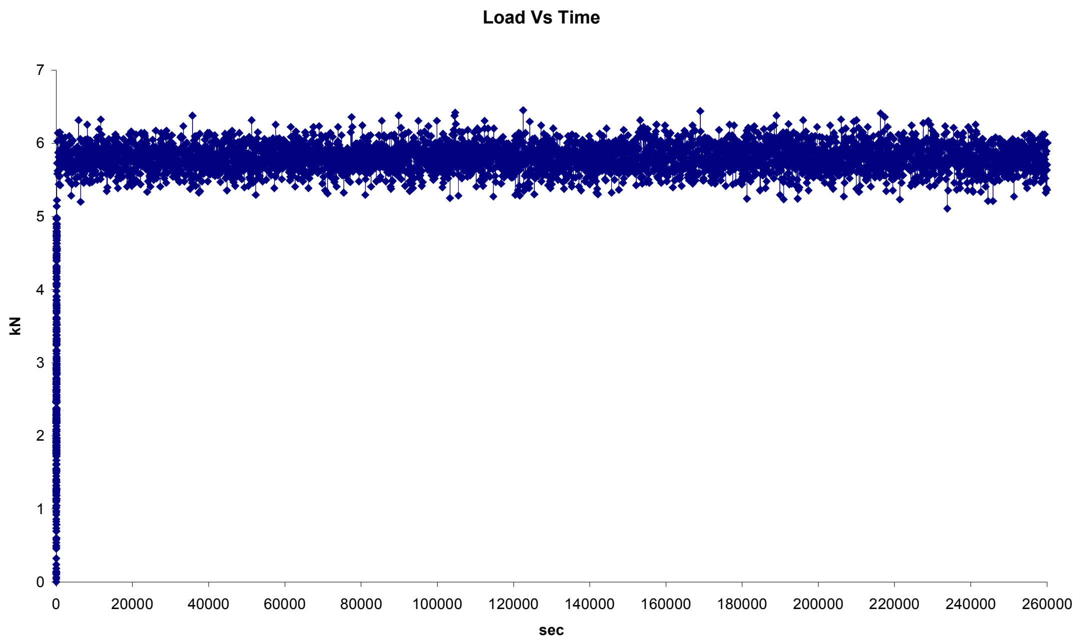

Figure 6: Load-time characteristic for sandstone rock sample

Scanning Electron Microscope Observations

The characteristics of the fracture surfaces were examined by means of an SEM, focusing mainly on the fracture initiation. An outline of the results shows that two types of cracks were observed.

(a).Intergranular cracks/Grain boundary cracks

Figures 7(a) to (f) show intergranular cracks which have initiated and propagated along grain boundaries. The preparatory stage of grain-boundary cracking can be seen clearly in Figures 7(a) and (e), which confirm that the chains of small cracks lie along grain boundaries. Similar chains of cracks are shown particularly in Figures 8(a) and (e) and in these cases the crack openings are larger and the cracked sections of the grain boundaries are easily identified.

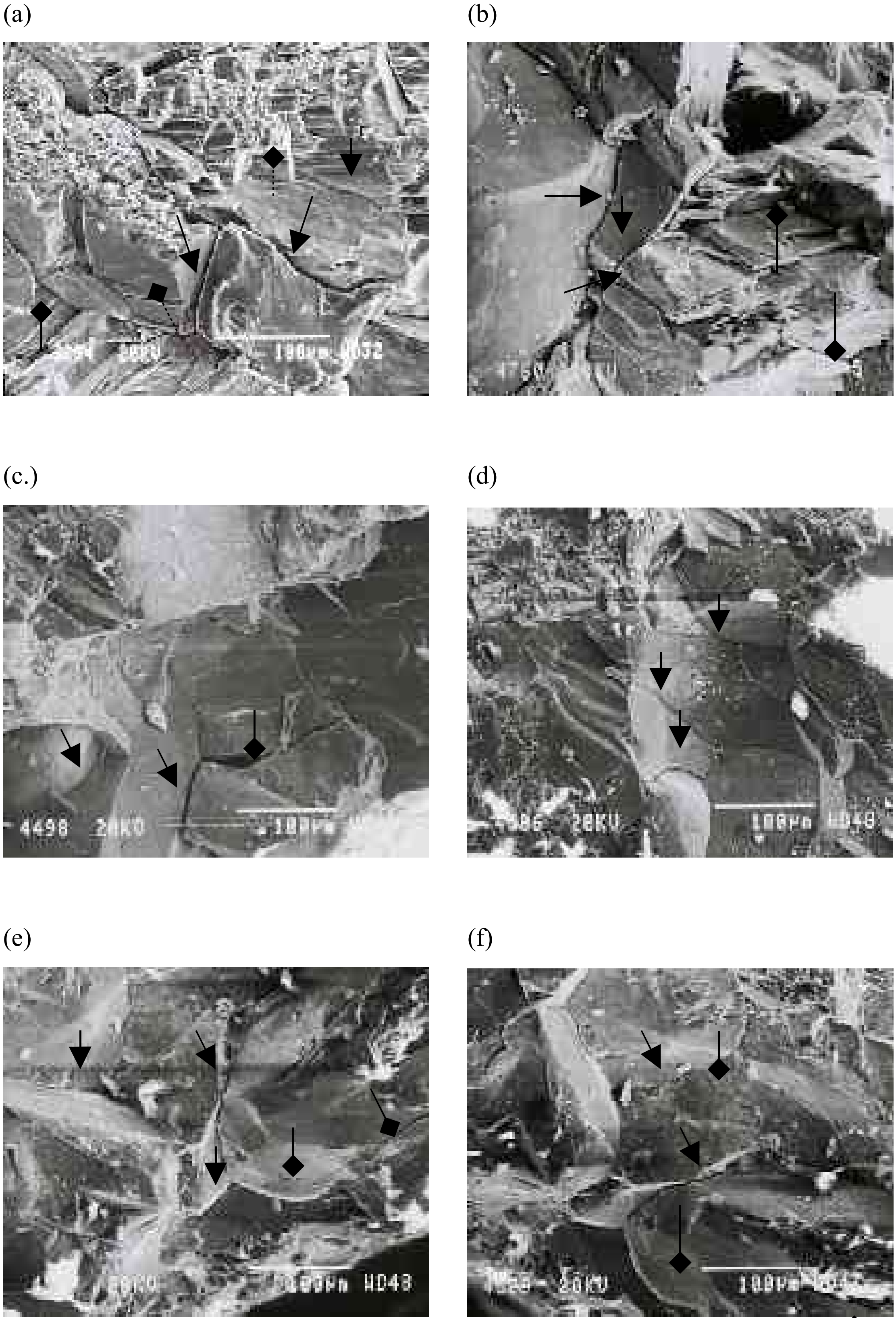

Figure 7: SEM micrograph illustrating general initiation and propagation of Inter-granular ( ) and Intra-granular ( ) cracks in anorthosite samples stressed 0.2UCS uniaxially

(a) (b)

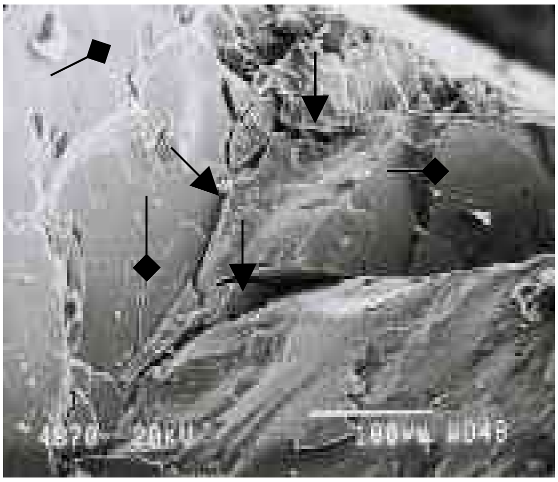

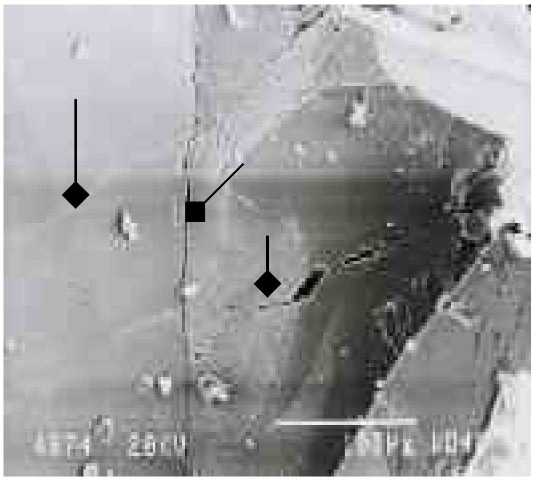

(c) (d)

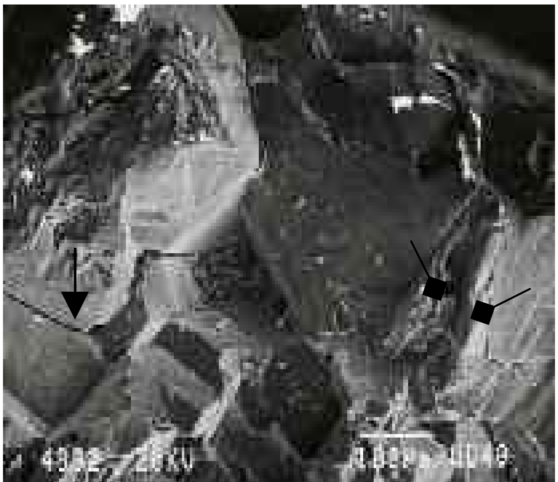

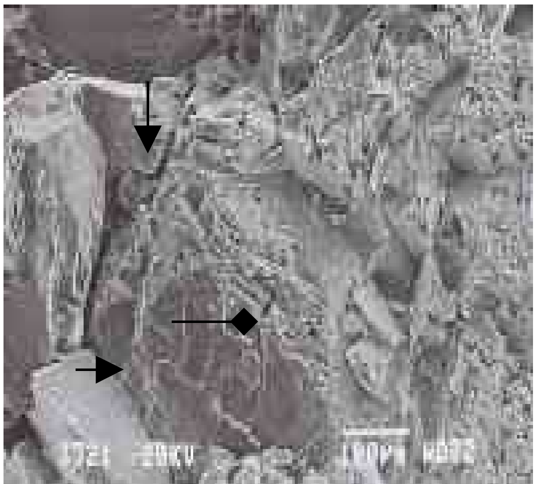

(e) (f)

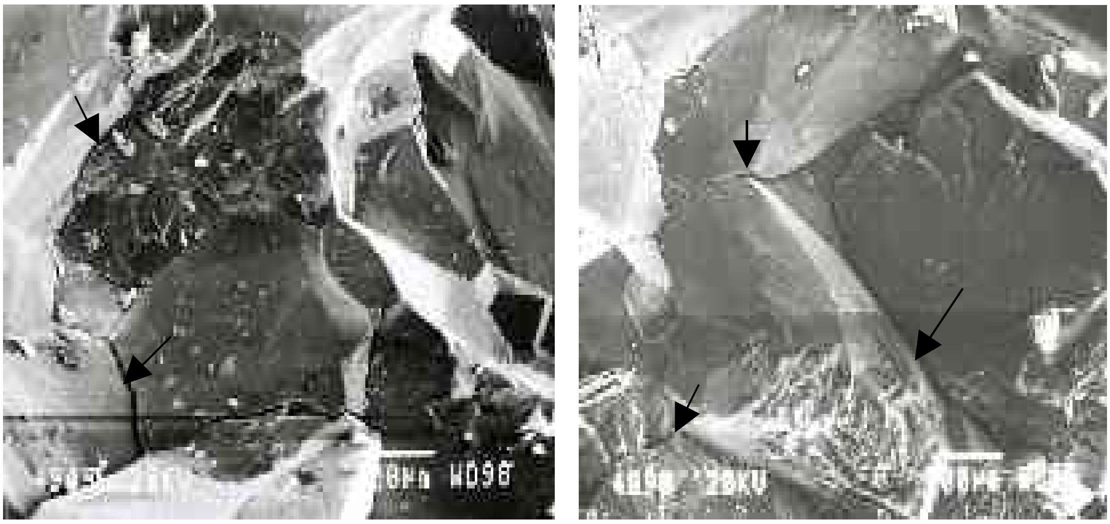

Figure 8: SEM micrograph illustrating general initiation and propagation of Inter-granular ( ) and Intra-granular ( ) cracks in anorthosite samples stressed to 0.4UCS uniaxially

(a) (b)

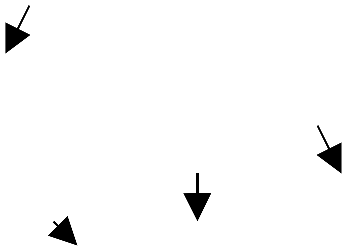

Figure 9: SEM micrograph illustrating general initiation and propagation of Inter-granular ( ) cracks in Sandstone samples stressed to 0.2UCS uniaxially

Intragranular cracks/Cracks passing through grains

These kind of cracks cut across/through mineral grains, and they appear commonly in groups parallel to each other as shown in Figure (10)

(a)

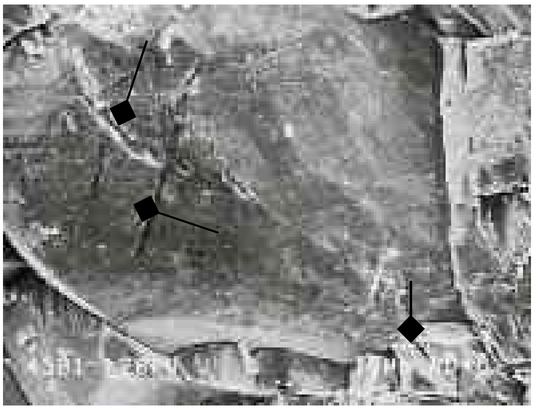

(b)

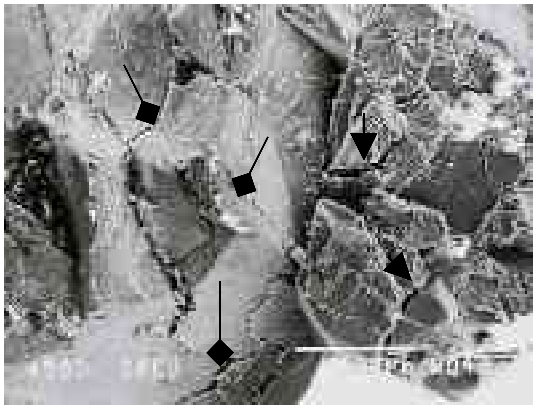

(c)

(d)

Figure 10: SEM micrograph illustrating general initiation and propagation of Inter-granular ( ) and Intra-granular ( ) cracks in Anorthosite samples stressed to 0.2UCS uniaxially

(a)

(b)

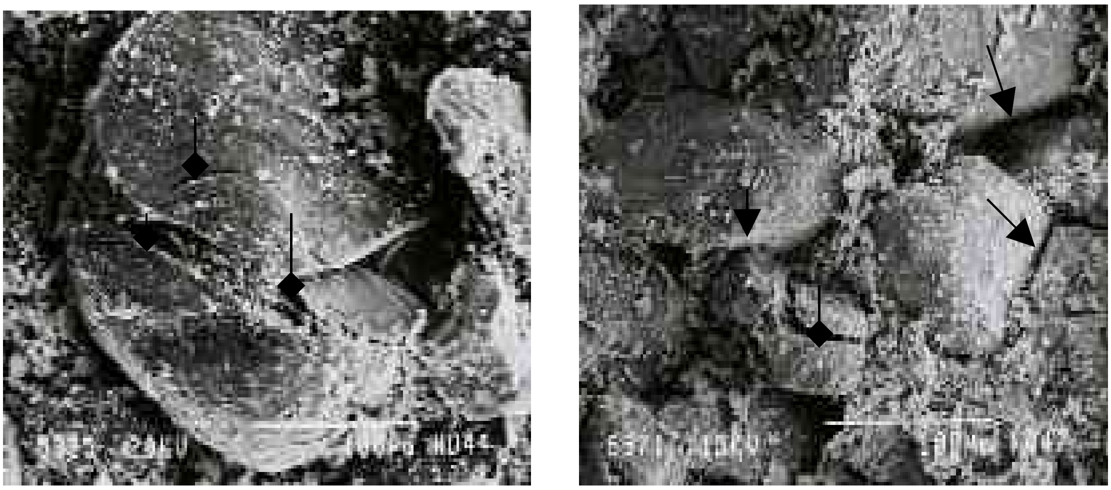

Figure 11: SEM micrograph illustrating general initiation and propagation of Inter-granular ( ) and Intra-granular ( ) cracks in Sandstone samples stressed to 0.2UCS uniaxially

Conclusions

SEM observations give a more detailed insight into the complex fracture behaviour that occurs in anorthosite and sandstone rock samples. These fractures were both intergranular and intragranular. The majority of the intragranular fractures are aligned with the direction of the applied stress.

The intragranular fractures grow in a manner typical of Griffith cracks propagating under compressive stresses conditions, the initial crack may form at a small angle to the direction of the applied stress and then propagates roughly parallel to the applied compressive stress, eventually terminating at the grain boundary [Figure10 (b) and (c]. However, the detailed study of specimens using the scanning electron microscope has shown that the prior existence of nucleating flaws or discontinuities (larger than the Griffith cracks) may not always be a necessary pre-requisite for the initiation and propagation of fractures.

References

BIENIAWSKI, Z.T. (1967a), Mechanism of brittle fracture of rock. Part I, Theory of fracture process, Int. J. Rock Mech. Min. Sci.,Vol 4, pp 395-406.

BIENIAWSKI, Z.T. (1967b), Mechanism of brittle fracture of rock. Part II, Experimental Studies, Int. J. Rock Mech. Min. Sci., Vol 4, pp 407-423.

BRACE,W.F. and BOMBOLAKIS, E.G. (1963), A note on brittle crack growth in compression, Int. J. Geophys. Res., Vol 68, pp 3709-3713.

International Society for Rock Mechanics (ISRM),(1979), Suggested Methods for determining the Uniaxial compressive strength and deformability of rock materials. Int. J. Rock Mech. Min. Sci., Vol 16, pp 135-140.

MARTIN, C.D. and CHANDLER, N.A. (1994), The Progressive fracture of Lac du Bonnet Granite, Int. J. Rock Mech. Min. Sci., Vol 31, No 6, pp643-659.

STACEY, T.R. and YATHAVAN, K. (2003), Examples of fracturing of rock at very low stress levels, Proc, 10th Int. Cong. Int. Soc. Rock Mech., Technology Roadmap for Rock Mechanics, S. Afr. Inst. Min. Metall., Vol 2, pp 1155-1159.